Hydrothermal-electrochemical codeposited hydoxyapatite/yttria-stabilized zirconia composite coating

X. F. XIAO
College of Materials Science & Engineering, Yanshan University, Qinhuangdao 066004, People's Republic of China; College of Chemistry and Material Science, Fujian Normal University, Fuzhou 350007, People's Republic of China

R. F. LIU*
College of Chemistry and Material Science, Fujian Normal University, Fuzhou 350007, People's Republic of China
E-mail: rfliu@vip.sina.com

Y. Z. ZHENG
College of Materials Science & Engineering, Yanshan University, Qinhuangdao 066004, People's Republic of China

Published online: 12 April 2006

Hydroxyapatite(HA)/yttria-stabilized zirconia(YSZ) composite coatings were deposited on titanium substrates using a hydrothermal electrochemical method in an electrolyte containing calcium, phosphate ions and YSZ particles. HA/YSZ composite coatings were prepared in different conditions with different electrolyte temperatures(100 $\sim$ 200°C), current densities(0.1 $\sim$ 10.0 mA/cm^2), and particles content in bath(0 $\sim$ 100 g/L). The effect of YSZ additions on the phase composition, microstructure, thermal stability, corrosion behavior and the bonding strength of HA/YSZ composite coatings were studied. The results show that crystallinity of HA in HA/YSZ composite coatings increase continuously with the electrolyte temperature and close to stoichiometric HA. The n(Ca)/n(P) ratio at 200°C is about 1.67 according with stoichiometric HA. YSZ particles are imbedded uniformly between the HA crystals. The average HA crystal size are reduced owing to the additions of YSZ particles. After annealing at 1200°C, tetragonal phase YSZ tend to react with the released CaO to form cubic phase YSZ and $CaZrO_3$, which cause destabilization of HA to decompose into more α-TCP phase. The bonding strength between HA/YSZ composite coatings and titanium substrates increase with increasing volume content of YSZ in the composite coatings (V %). HA/YSZ composite coatings exhibit a better electrochemical behavior than pure HA coatings and uncoated Ti metals.

1. Introduction

Hydroxyapatite($Ca_{10}(PO_4)_6(OH)_2$, HA) is considered as the bioceramic material that has favorable osteoconductive and bioactive properties which promote rapid bone formation and strong biological fixation to bony tissue [1, 2]. However, its mechanical properties of low strength and high brittleness restrict the application only in nonload-bearing areas of the human body. One way to solve these problems is to apply HA coatings onto biocompatible metal substrates so as to achieve the necessary mechanical strength and bioactive properties at the same time [3]. Currently, the most widely applied coating procedure is the plasma spray technique. The major problems for this technique are that it is a line of sight process that produces non-uniform coating with heterogeneous structure, and the high temperatures causes the decomposition and phase transformation of HA during the spray coating process [4, 5].

*Author to whom all correspondence should be addressed.
0022-2461
DOI: 10.1007/s10853-005-5340-y

Electrochemical deposition of HA coating has recently attracted considerable attention because of a variety of advantages, such as a low process temperature, the ability to deposit on porous or complex shapes of substrates, the microstructure of coatings can be regulated by controlling the composition of the electrolyte, the electrolyte temperature, the current density, the current loading time and the composition of the substrate metal, the crystallinity of deposits increased with the electrolyte temperature [6–9]. Based on these results, Ban S [10, 11] employed hydrothermal-electrochemical method for HA coatings above 100°C in an electrolyte. Needle-like HA were synthesized under different deposition conditions. The size of needle-like HA remarkably increased with the electrolyte temperature and current loading time, and slightly changed with current density. However, our previous studies reported that the bonding strength between HA coatings and titanium substrates produced by the hydrothermal-electrochemical method are weak [12]. This major drawback limits the application potential of hydrothermal-electrochemical method. The present work is aimed at improving the bonding strength of HA coating by modifying the hydrothermal-electrochemical process. This is done by adding yttria stabilized zirconia (YSZ) in the electrolyte so that the HA and YSZ could be codeposited on titanium substrates.

ZrO_2, especially YSZ, having the attributes of high strength and stress-induced phase transformation toughening, has been used to strengthen the brittle materials [13, 14]. Biocompatibility is another crucial merit of ZrO_2 [15]. There are a variety of processing routes for preparing HA/ZrO_2(or HA/YSZ) composite coatings, examples of which can be seen in the sintering method [16] and the electrochemical method [17]. Thermal spray techniques (plasma spray and high velocity oxy-fuel) are employed to produce composite coatings because of their high thermal efficiency and relative economy [18–20]. However, due to the high temperature of thermal spray techniques, HA tends to decompose and lose some of its bioactive properties.

This paper presents HA/YSZ coatings produced via hydrothermal-electrochemical method. This method belongs to the so-called soft solution processing (SSP) [21, 22], offering the advantage of enhanced purity, lower reaction temperature and higher film growth rate. It is expected that a synergistic effect of codeposition of HA and YSZ might exhibit improved bonding strength, with better bioactivity. The effect of operating conditions on the volume percent of YSZ in the composite coatings are examined. The microstructure, phase composition, thermal stability, corrosion behavior and the bonding strength of composite coatings are investigated.

2. Materials and methods

2.1. Coating preparation

The experiments were carried out in a stainless steel autoclave with a Teflon liner (inner volume: 200 mL). The autoclave was equipped with outlets for connection of three electrode [23]. Titanium metal substrates of 99.9% purity and dimensions of 10 mm × 100 mm × 0.5 mm were used as working cathodic electrodes, and a platinum foil served as a counter electrode. The reference electrode was an anodized Ag wire. The wire was first anodized in a KCl solution, rinsed and placed in a fritted glass tube filled with the electrolyte [24]. All potentials were referred to this reference electrode. Before deposition the working electrode surface was polished with abrasive paper, etched in 4% HF solution for 4 min, ultrasonicated in acetone for 10 min, then washed with deionized water and dried in air. The temperature in the autoclave was regulated using an external heating system, a chromel-alumel thermocouple and an automatic controller. The electrolyte used for deposition of coatings contained 0.0105 mol/L $Ca(NO_3)_2$, 0.0063 mol/L $NH_4H_2PO_4$, and with or without 0∼100 g/L commercially 3 mol% yttria-stabilized zirconia (YSZ) particles (typical size: 1.0–5.0 μm). $NaNO_3$ ($[NO_3^-] = 0.1$ mol/L) was also added to improve the ionic strength of the electrolytes. YSZ was supplied by China Medicine Shanghai Chemical Reagent Corporation. YSZ were kept in suspension in the electrolyte by a magnetically driven Teflon coated stirring bar. The electrolyte were prepared with regent grade chemicals and deionized water. The pH of the electrolyte was adjusted to 4.60 at 25°C by the addition of dilute ammonia water. At any time, 150 ml of electrolyte was sealed in the autoclave with 75% compactedness. The hydrothermal-electrochemical deposition was carried out in galvanostat mode, the current density of the cathode was maintained at a predetermined value range from 0.1 to 10.0 mA/cm^2. Temperature was carried out at a fixed temperature between 100 and 200°C for 120 min. After deposition, the coatings were rinsed with deionized water and dried in air.

2.2. Coating characterization

The weight of coatings were determined from the weight change of the substrates before and after deposition. The content of YSZ particles in composite coatings was measured gravimetrically by dissolving the coating in diluted HCl solution, filtering through weighted membrane filter paper and then calculating volume percent of YSZ in the coatings. Inductively coupled plasma emission spectroscopy(ICP) was used to measure the concentration change of Ca^{2+} ions after adding YSZ in the electrolyte for 2 h. The Philips XL30 Environmental Scanning Electron Microscope (ESEM) equipped with Philips Energy Dispersive X-ray Analyzer (EDX) was used to study the microstructure characterization and elemental analyses of HA/YSZ composite coatings. Phase analysis was performed on the Philips X'Pert MPD X-ray diffractometer system (XRD) using Cu*Ka* radiation at 40 kV and 30 mA. Nicolet Avatar 360 Fourier transform infrared spectroscopy(FTIR) was used to determine the chemical composition of the coatings. The bond

strength of HA/YSZ composite coatings (σ_b) was evaluated using standard tensile adhesion test (ASTM-C633) for hydrothermal-electrochemical codeposited coatings. Two identical cylindrical Ti substrates were used as a set, one rod was first sand-blasted and hydrothermal-electrochemical codeposited with a HA/YSZ composite coating. The coupling rod was also sand-blasted, glued with thermoplastic and then joined under pressure in a fixture to the rod with HA/YSZ coating. The couples, cured at 190°C for 2 h, were subjected to tensile tests at an extension rate of 1 mm/min until failure. For each testing material, five specimens were used, and the bonding strength data is reported as the average values.

To observe the corrosion behavior of the HA/YSZ, a potentiodynamic polarization test was conducted using a potentiostat (model DJS-292, Shanghai Rex Instruments, China) in physiological saline solution (0.9%NaCl) at 37°C. Anodic polarization curves were obtained by scanning the potential from –1.0 V below the corrosion potential up to 2.0 V at a scan rate of 5 mV/s.

3. Results and discussion

3.1. Phase composition

Fig. 1 shows the XRD patterns for the composite coatings prepared at temperature 100, 140, 160 and 200°C. Diffraction peaks due to titanium substrate, HA and YSZ are observed in all the patterns. It is clear that the composite coatings consist of HA and YSZ without other phases being detected. XRD analysis at high 2θ angle (68–78°) confirm that the YSZ is a pure tetragonal phase ZrO_2(t-ZrO_2) according to JCPDS card for t-ZrO_2 (JCPDS 88–1007). Broad diffraction peaks are observed for the HA prepared at low temperature (100°C). With the increase in electrolyte temperature these diffraction peaks become sharp and the intensity of the (002) plane become strong, indicating the increase in crystallinity of HA in the coatings. In order to estimate the crystallinity of HA in each coatings, the inverse of full width at half maximum(FWHM) breadths was calculated from (300) and (002) diffraction peak as representations of the a- and c-axis. The evaluated crystallinity of HA are given in the Table I. The results show that a strong dependence of the crystallinity of HA on the electrolyte temperature. It seems that the crystallinity of the HA formed using the hydrothermal–electrochemical method at 200°C is similar to that of the fired HA at 900°C under atmospheric pressure from the amorphous phase [10].

TABLE I The inverse of FWHM of HA/YSZ prepared at different temperature

Temperature/°C	(002)	(300)
100	Immeasurable	Immeasurable
140	4.87	4.23
160	5.45	5.12
200	7.30	7.31

Fig. 2 show FTIR spectra of the composite coatings formed at 100, 140, 160 and 200°C. The spectra show the absorption bands characteristic for HA, largely reported in the literature [25]. So, the stretching and librational modes of the OH^- groups appear at: ν_s(3570 cm^{-1}) and ν_L(632 cm^{-1}), whereas the internal modes corresponding to the PO_4^{3-} groups occur at: ν_3(1095 and 1031 cm^{-1}), ν_1(960 cm^{-1}), ν_4(605 and 565 cm^{-1}) and ν_2(470 cm^{-1}). Molecular and adsorbed water bands are discerned at 1632 and 3440 cm^{-1}. Also, one additional band of low intensity centered around 865 cm^{-1} can be observed. CO_3^{2-}(type B) or PO_4H^{2-} groups could be responsible for this band. However, CO_3^{2-} type B presents typical bands in the region 1500–1400 cm^{-1}, which are not observed in our case. So, only the HPO_4^{2-} groups appear to be responsible for the band. According to the chemical formula of HA ($Ca_{10}(PO_4)_6(OH)_2$), HA have no HPO_4^{2-} groups. The presence of the HPO_4^{2-} groups indicate the formation of nonstoichiometric HA. The EDX analyses show that the elements of the composite coatings are calcium,

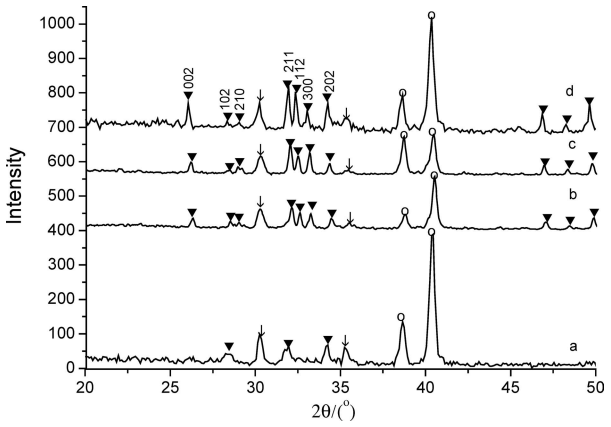

Figure 1 XRD patterns of the HA/YSZ on the titanium substrate after loading of a constant current at 0.3 mA/cm^2 at different temperature: a. 100°C b. 140°C c. 160°C d. 200°C. Legend: (▼)HA, (↓)t-ZrO_2, (○)Ti.

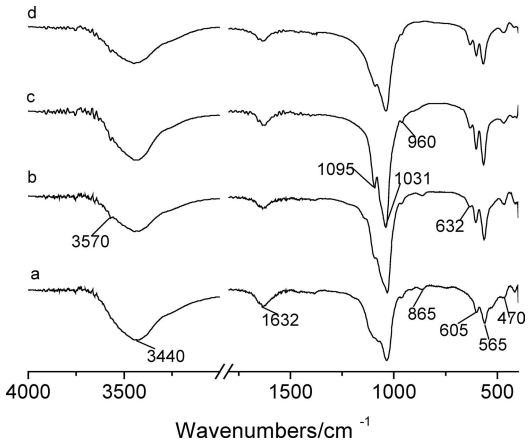

Figure 2 FTIR spectra of the HA/YSZ after loading of a constant current at 0.3 mA/cm^2 at different temperature: a. 100°C b. 140°C c. 160°C d.200°C.

phosphorus, oxygen and zirconium without other elements detected. The n(Ca)/n(P) molar ratio of composite coatings are determined to be 1.55 ± 0.03, 1.60 ± 0.03, 1.63 ± 0.02 and 1.67 ± 0.01, respectively. Since the HA has a nominal n(Ca)/n(P) ratio of 1.67, it is manifest that the HA prepared by hydrothermal-electrochemical are calcium-deficient hydroxyapatite ([usually expressed as $Ca_{10-x}(PO_4)_{6-x}(HPO_4)_x(OH)_{2-x}$, CDHA] [26]. The n(Ca)/n(P) ratio increase with increasing electrolyte temperature, the n(Ca)/n(P) ratio at 200°C is about 1.67, according with stoichiometric HA. Furthermore, with the increase in electrolyte temperature the intensity of absorption bands of OH^- groups become strong, and the intensity of absorption bands of HPO_4^{2-} groups become weak and disappear at 200°C, and the absorption peaks due to PO_4^{3-} show stronger intensities and split more clearly. These results suggest that the crystallinity of composite coatings increase continuously with the electrolyte temperature and close to stoichiometric HA.

3.2. Microstructure of coatings

The ESEM observations of HA/YSZ composite coatings and pure HA coatings without YSZ particles deposited at 100,140,160 and 200°C are shown in Figs 3a–e and f–i, respectively. Two distinctive features can be seen in the Fig. 3a–e, the small particles are YSZ and the needle-like crystals are HA which having a defined hexagonal crystal habit. Fig. 3f–i show that the width and the length of HA crystals increase with the electrolyte temperature,

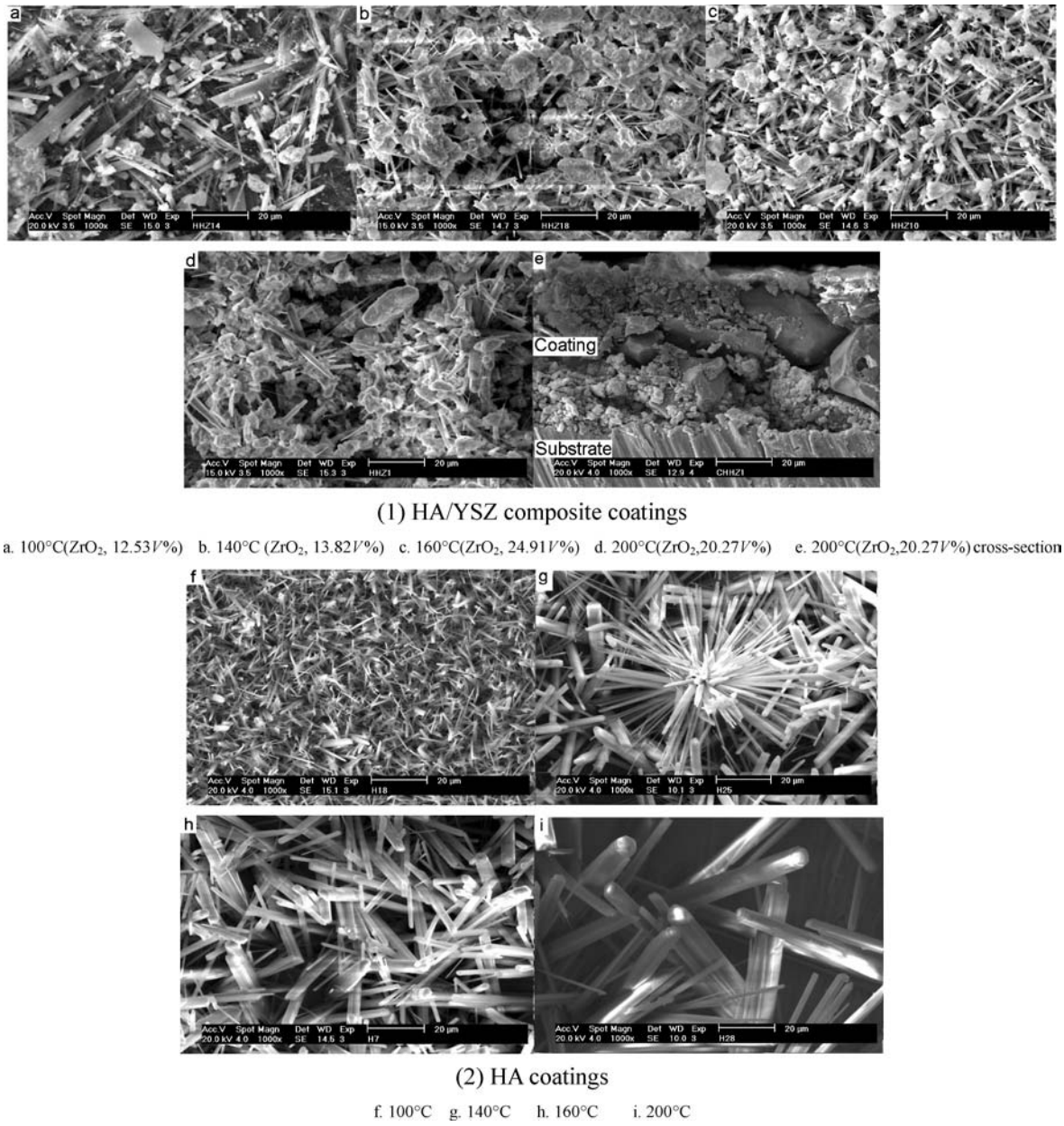

Figure 3 ESEM micrographs of the coatings after loading of a constant current at 0.3 mA/cm^2 at different temperature.

but the numbers of needle-like HA crystals decrease with the electrolyte temperature. Although the needle-like HA crystals shown are in a random orientation, there is a possibility that they firstly grow as needles of different sizes, radially pointing out from a center of the cluster which act as the nucleation site (Fig. 3 g). It can be seen that the average size of HA crystals in the HA/YSZ composite coatings are much smaller than that in the pure HA coatings, indicating the function of YSZ particles as an HA crystal growth inhibitor during hydrothermal-electrochemical deposition. The reason may be that YSZ particles are absorbed on the surface of HA crystals and hinder the growth of crystals. Fig 3 (e) shows the SEM image of a cross-section of HA/YSZ composite coating. It revealed that the YSZ particles are embedded uniformly between the HA crystals.

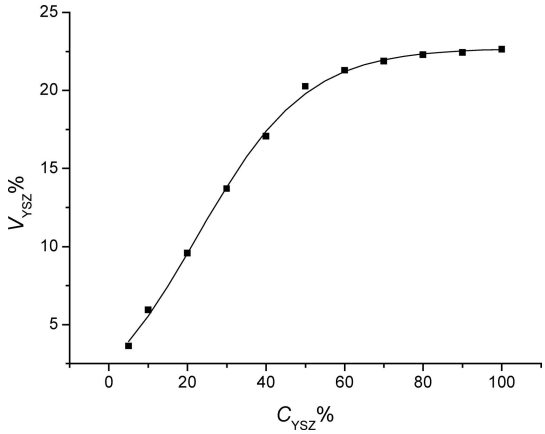

Figure 4 Relationship between YSZ concentration in electrolyte and the content of YSZ in the composite coatings (V%). $T = 200°C$, $i = 0.3$ mA/cm^2.

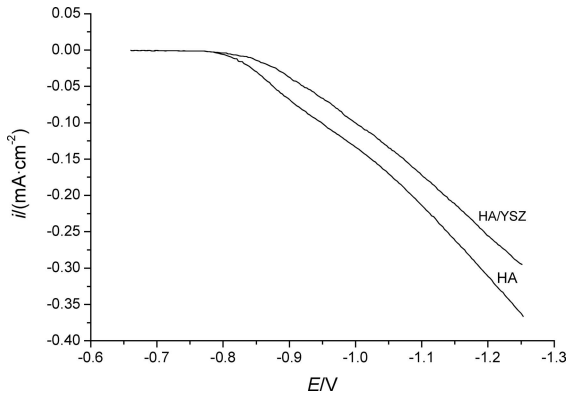

Figure 5 Cathodic polarization curves for deposition of HA and HA/YSZ. $T = 200°C$, 50 g/L YSZ.

3.3. Codeposition process

A previous paper demonstrated that the electrochemical deposition of HA on Ti substrates occursc through a nucleation and growth mechanism [7]. In general, the formation of HA on the cathode is initiated once the level of supersaturation exceeds the critical level required for the nucleation of HA. During the electrochemical deposition process, the pH of the electrolyte in the close vicinity of the cathode is increased as a result of the electrolysis. This causes the supersaturation level to raise and thus HA may precipitate on the cathode surface due to accumulation of Ca^{2+}, $PO_4{}^{3-}$ and OH^-. These results suggest that the diffusion process is a rate-determining step in the electrochemical deposition of HA, therefore, increasing electrolyte temperature is in favor of the crystal growth of HA.

The concentration of Ca^{2+} in electrolyte decreases from 0.0105 mol/L to 0.0097 mol/L after adding 50 g/L YSZ particles for 2 h, which revealed that YSZ particles would adsorb Ca^{2+} ions and would be migrated and adsorbed onto the cathode surface for codeposition by electric field and stirring action. Fig. 4 shows the relationship between concentration of YSZ particles in the electrolyte and the volume content of YSZ in the composite coatings($V\%$). It can be noted that YSZ in the coatings increases with an increase of YSZ in the electrolyte, tending to attain a steady value at YSZ concentration of about 80 g/L. Moreover, the curve is quite similar to the well known Langmuir adsorption isotherms, supporting a mechanism based on an adsorption effect. The codeposition of YSZ may be attributed to the adsorption of YSZ particles on the cathode surface, as suggested by Guglielmi's two-step adsorption model [27]. Once the particle is adsorbed, HA crystals begin building around the cathode slowly, encapsulating and incorporating the particles. The plateau observed at higher particles concentration in eletrolyte may be a result of saturation in adsorption on cathode surface.

The cathodic polarization behavior of hydrothermal-electrochemical deposition with and without YSZ additional particles is shown in Fig. 5. It indicates that the YSZ particles in the electrolyte cause an increase in the cathodic polarization, but the slope is unchanged. This means that the adsorption of YSZ particles on cathode surface hinders the deposition of HA, but does not significantly affect the electrochemical reaction mechanism.

The relationship between current density and $V\%$ is shown in Fig. 6. An increase in current density from 0.1 mA/cm^2 led to an increase in $V\%$. A further increase in current density led to a decline in $V\%$, as shown in Fig. 6. In the region below 2.0 mA/cm^2, the increasing $V\%$ can be attributed to the increasing tendency for absorbed YSZ particles to arrive in the cathode surface, which is consistent with Guglielmi's model. In this case, the codeposition behavior of particle-adsorption-controlled and the particle deposition is dominant. When current density is greater than 2.0 mA/cm^2, the decreasing trend can be explained by the fact that an increase in current density results in a more rapid deposition of HA crystals due to the more quickly reduction of H_2O, and less YSZ particles are embedded in the composite coatings due to a detrimental effect of hydrogen evolution on codeposition of YSZ particles. Hence, in this case the HA crystals deposition dominates the codeposition process.

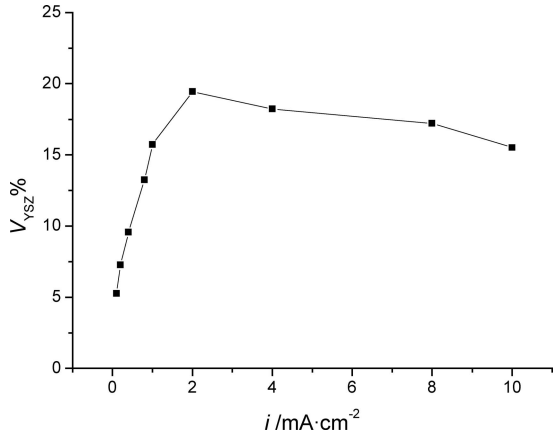

Figure 6 The effect on current density on the content of YSZ in the composite coatings (V%).

Hydrogen molecule formed on the cathode would coalesced into gaseous macroscopic bubbles. HA/YSZ cannot deposite at sites occupied by hydrogen bubbles because there is no mechanism for mass transport through this gas phase. When current density is greater than 5.0 mA/cm^2, the composite coatings are loose and porous and easily scaled off the substrates.

3.4. Thermal stability

The XRD patterns of the HA/YSZ composite coatings removed mechanically after heat treatment at various temperatures for 2 h are shown in Fig. 7. With the annealing temperature varying from 500°C to 1000°C, the tetragonal phase YSZ don't change into other phases. The absence of transformation of YSZ is beneficial to the coating since YSZ has high strength, high toughness and excellent resistance against impact. Especially for the implant coating, high toughness is important since the implant prosthesis must be reliable in the presence of body fluids and complex local loading. On the other hand, HA is stable up to 700°C, above which beta tricalcium phosphate (β-TCP) phase and CaO is transformed from the HA phase. After annealing at 1200°C for 2 h, the diffraction peak of HA and CaO phase have disappeared, and tetragonal phase change into cubic phase zirconia according the JCPDS card(JCPDS 49–1642), and the alpha calcium phosphate (α-TCP) phase could be identified apparently according the JCPDS card(JCPDS 70-0364). indicating the decomposition completely of HA. To further elucidate the results, the composite coatings were immersed in hydrochloric acid to dissolve the soluble α-TCP, and then the residues were collected and analyzed by XRD. It could be seen from Fig. 7 f that little $CaZrO_3$ are found. High-resolution examination of $2\theta = 68$–$78°$ range indicates that the crystal phase of particles is cubic phase zirconia, at $2\theta \approx 72.8°$ and 74.33°, doublets of respective tetragonal (400) and (004) planes do not appear [28]. It had been reported in the study of sintered bulk HA/ZrO_2 composite [29] that HA tended to release CaO and transform into β-TCP, and at higher annealing temperature, into α-TCP. Moreover, zirconia, initially in the tetragonal phase, tended to react with the released CaO to form cubic zirconia or $CaZrO_3$. Therefore, the decomposition of HA and reaction between HA and zirconia after annealing at 1200°C can be expressed as follows:

$$Ca_{10}(PO_4)_6OH_2 \rightarrow 3\alpha{-}Ca_3(PO_4)_2{+}CaO + H_2O$$

$$x[t{-}ZrO_2{+}CaO] \rightarrow x[c - ZrO_2]$$

$$(1-x)[CaO + t - ZrO_2] \rightarrow (1-x)[CaZrO_3]$$

HA decompose into α-TCP and CaO firstly, and then some CaO will dissolve into zirconia and form a solid solution, then produce a phase change from tetragonal to cubic, others CaO will react with YSZ to from $CaZrO_3$, meanwhile these reaction cause destabilization of HA to decompose into more α-TCP phase.

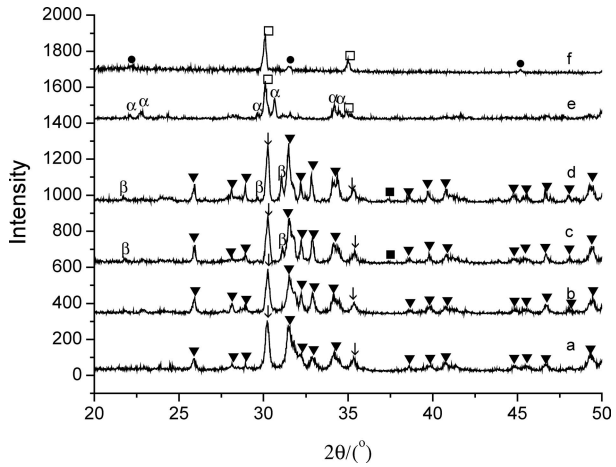

Figure 7 XRD patterns of HA/YSZ (ZrO_2, 20.27 V%) composite coatings codeposited at 200°C and 0.3 mA/cm^2 after annealing for 2 h at different temperature: a. 500°C b. 700°C c. 800°C d. 1000°C e.1200°C f. residues of HA/YSZ composite coating after sintering at 1200°C for 2 h and immersed in hydrochloric acid. Legend: (▼)HA, (↓)t-ZrO_2, (β) β -TCP, (□) c-ZrO_2,(α) α -TCP,(●)$CaZrO_3$, (■)CaO.

3.5. Bonding strength

Adding ZrO_2 as second phase to HA aim at improving the bonding strength between the coatings and the substrates. The results of bonding strength of HA/YSZ composite coatings after annealing at 500°C for 2 h were shown in Fig. 8. The following conclusions can be drawn from the measurements: (1) the pure HA coating shows the lowest bonding strength; (2) the bond strength of the composite coatings have been improved by the additions of YSZ and increase with an increase in YSZ content. The strengthening mechanism of hydroxyapatite-electrochemical codeposited HA/YSZ composite

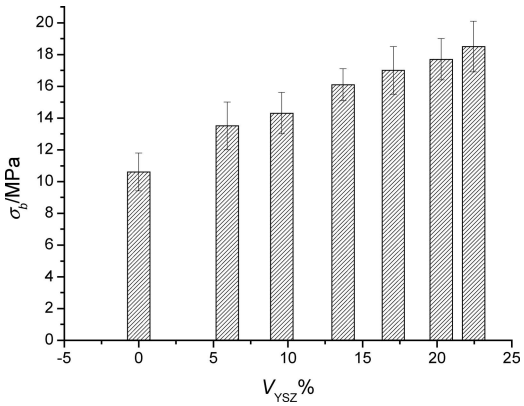

Figure 8 Relationship between the bonding strength of coatings and the content of YSZ in the coatings.

coatings should not relate to transformation toughening of YSZ particles, but to homogeneous distribution of YSZ particles in the HA. Other factors of microstructure, such as HA crystal size will certainly influence the bonding strength of coatings. The less HA crystal size due to the addition of YSZ will increase the bonding strength of the coatings. Furthermore, it was reported that the adhesion of HA coating on Ti substrate could be improved by a reduction of the coefficient of thermal expansion (CTE) of the coating with an incorporation of 60% TiO_2 [30]. It was reported that the CTE of HA was 15×10^{-6} K^{-1} and that of ZrO_2 and Ti were 10×10^{-6} K^{-1} and 8.6×10^{-6} K^{-1}, respectively. It is also likely that the CTE of HA/YSZ composite coating are smaller than that of HA coatings.

3.6. Corrosion test

The potentiodynamic polarization curves of the pure HA coating, HA/YSZ composite coating and Ti metal are plotted in Fig. 9. Before corrosion test, Ti metal was subjected to the same hydrothermal electrochemical process with HA/YSZ composite coating in an elecrolyte without reactive ions/particles but with controlled pH. The results show that the pure HA coating indicates highest corrosion potential and a passive region between 0.10 and

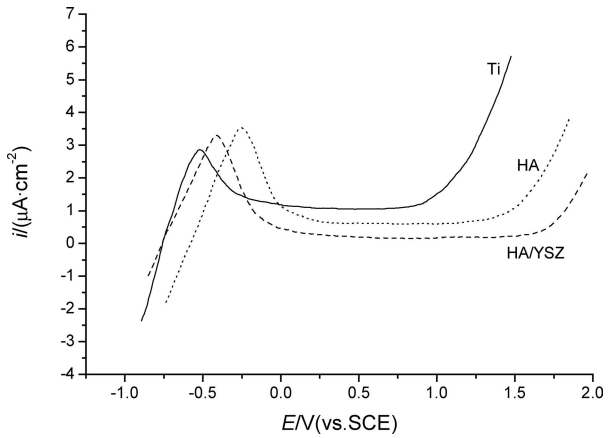

Figure 9 Potentiodynamic polarization curves of samples.

1.45 V with a current density of about 0.59 μA/cm^2; The HA/YSZ composite coating possesses wider passive region and the lowest corrosion current about 0.12 μA/cm^2. The results confirm that HA/YSZ composite coating exhibits a better electrochemical behavior than pure HA coating possibly due to less crystal size and the better cohesion degree of the coating. However, the Ti metal gives the lowest corrosion potential and the highest corrosion current. Therefore, all coatings on Ti metal do exhibit significantly improve corrosion resistance compared to the hydrothermally treated Ti metal.

4. Conclusion

HA/YSZ composite coatings were successfully prepared by hydrothermal-electrochemical codeposited method. The phase composition, microstructure, thermal stability, bonding strength and corrosion behavior of the composite coatings were studied and the results are summarized as follows:

(1) The crystallinity of the HA in the coatings increased continuously with increasing electrolyte temperature and closed to stoichiometric HA. The average grain size of HA in the HA/YSZ composite coatings was reduced compared with that in the pure HA coating, indicating the function of the YSZ particles as an HA grain growth inhibitor.

(2) The YSZ volume content in the coatings increase with an increase of YSZ content in the electrolyte, and increase with the increasing current density from 0.1–2.0 mA/cm^2 and decrease with the current density beyond 2.0 mA/cm^2.

(3) Tetragonal YSZ phase remain stable when HA/YSZ composite coating annealed below 1000°C. HA decompose into β-TCP and CaO as the temperature increased from 800°C to 1000°C. After annealing at 1200°C, tetragonal phase tend to react with the released CaO to form cubic phase zirconia and $CaZrO_3$, meanwhile this reaction causes destabilization of HA to decompose into more α-TCP phase.

(4) The bonding strength between HA/YSZ composite coatings and titanium substrates increase with increasing volume content of YSZ in the composite coatings($V\%$). The strengthen mechanism were associated with the YSZ uniformly dispersion and less HA crystal size.

(5) HA/YSZ composite coatings exhibit a better electrochemical behavior than pure HA coatings and the hydrothermally treated Ti metal.

Hydrothermal-electrochemical codeposition method provides an opportunity to prepare high performance HA/YSZ composite coatings for bone prosthesis. The bioactivity and biocompatibility evaluation of the composite coatings are being studied by soaking the coatings in simulated body fluid and testing cell proliferation experiment on the surface of the composite coatings *in vitro* now.

Acknowledgment

The work was supported by Natural Science Foundation of Fujian Province of China (No. 2000F003)

References

1. G. L. DARIMONT, R. CLOOTS and E. HEINEN *et al., Biomaterials.* **23** (2002) 2569.
2. M. YOSHINARI, Y. ODA and T. INOUE *et al., ibid.* **23** (2002) 2879.
3. A. K. LYNN and D. L. DUQUESNAY, *ibid.* **23** (2002) 1937.
4. J. I. HUAXIA, C. B. PONTON and P. M. MARQUIS, *J. Mater. Sci. Mater. Med.* **3** (1992) 283.
5. R. Y. WHITEHEAD, W. R. LACEFIELD and L. C. LUCAS, *J. Biomed. Mater. Res.* **27** (1993) 1501.
6. M. SHIRKHANZADEH, *J. Mater. Sci. Lett.* **10** (1991) 1415.
7. M. SHIRKHANZADEH, *J. Mater. Sci. Mater. Med.* **9** (1998) 67.
8. M. KUMAR, H. DASARATHY and C. RILEY, *J. Biomed. Mater. Res.* **45** (1999) 302.
9. M. MANSO, C. JIMENEZ and C. MORANT *et al., Biomaterials* **21** (2000) 1755.
10. S. BAN and S. MARUNO, *J. Biomed. Mater. Res.* **42** (1998) 387.
11. S. BAN and J. HASEGAWA, *Biomaterials.* **23** (2002) 2965.
12. R. F. LIU, X. F. XIAO and L. Y. LIN *et al., Chem. J. Chin. Univ.* **25** (2004) 304.
13. B. Y. CHOU, E. CHANG and S. Y. YAO *et al., J. Am. Ceram. Soc.* **85** (2002) 661.
14. D. J. GREEN, *J. Am. Ceram. Soc.* **65** (1982) 610.
15. Y. W. GU, K. A. KHOR and D. PAN *et al., Biomaterials.* **25** (2004) 3177.
16. J. LI, H. LIAO and L. HERMANSSON, *ibid.* **17** (1996) 1787.
17. Y. M. SUNG, Y. K. SHIN and Y. W. SONG *et al., Crystal Growth Design* **5** (2005) 29.
18. C. S. YIP, K. A. KHOR and N. L. LOH *et al., J. Mater. Proc. Technol.* **65** (1997) 73.
19. H. LI, K. A. KHOR and R. KUMAR *et al., Surf. Coat. Technol.* **182** (2004) 227.
20. L. FU, K. A. KHOR and J. P. KIM, *ibid.* **140** (2001) 263.
21. Z. B. WU and M. YOSHIMURA, *Solid State Ionics* **122** (1999) 161.
22. M. YOSHIMURA, *J. Mater. Res.* **13** (1998) 796.
23. M. YOSHIMURA, W. URUSHIHARA and M. YASHIMA *et al., Intermetallic* **3** (1995) 125.
24. L. I. HILL, R. PORTAL and A. L. LA SALLE, *et al., Electrochem. Solid-State Lett.* **4** (2001) D1.
25. M. ANDRES-VERGES, C. FERNANDEZ-GONZALEZ and M. MARTINEZ-GALLEGO, *J. European Ceramic Society* **18** (1998) 1245.
26. S. C. LIOU, S. Y. CHEN and H. Y. LEE, *Biomaterials.* **25** (2004) 189.
27. G. WU, N. LI and D. R. ZHOU, *et al., Surf. Coat. Technol.* **176** (2004) 157.
28. R. C. GARVIE, R. H. HANNINK and R. T. PASCOE, *Nature.* **258** (1975) 703.
29. J. M. WU and T. S. YEH, *J. Mater. Sci.* **23** (1988) 3771.
30. X. B. ZHENG and C. X. DING, *J. Thermal Spray Technol.* **9** (2000) 520.

Received xxx
and accepted 12 July 2005